Comparative testing of four ionospheric models driven with GPS measurements

J. Feltens,[1] M. Angling,[2] N. Jackson-Booth,[2] N. Jakowski,[3] M. Hoque,[3] M. Hernández-Pajares,[4] A. Aragón-Àngel,[4] R. Orús,[5] and R. Zandbergen[6]

Received 30 November 2010; revised 16 March 2011; accepted 11 April 2011; published 28 July 2011.

[1] In the context of the European Space Agency/European Space Operations Centre funded Study "GNSS Contribution to Next Generation Global Ionospheric Monitoring," four ionospheric models based on GNSS data (the Electron Density Assimilative Model, EDAM; the Ionosphere Monitoring Facility, IONMON v2; the Tomographic Ionosphere model, TOMION; and the Neustrelitz TEC Models, NTCM) have been run using a controlled set of input data. Each model output has been tested against differential slant TEC (dSTEC) truth data for high (May 2002) and low (December 2006) sunspot periods. Three of the models (EDAM, TOMION, and NTCM) produce dSTEC standard deviation results that are broadly consistent with each other and with standard deviation spreads of ~1 TECu for December 2006 and ~1.5 TECu for May 2002. The lowest reported standard deviation across all models and all stations was 0.99 TECu (EDAM, TLSE station for December 2006 night). However, the model with the best overall dSTEC performance was TOMION which has the lowest standard deviation in 28 out of 52 test cases (13 stations, two test periods, day and night). This is probably related to the interpolation techniques used in TOMION exploiting the spatial stationarity of vertical TEC error decorrelation.

Citation: Feltens, J., M. Angling, N. Jackson-Booth, N. Jakowski, M. Hoque, M. Hernández-Pajares, A. Aragón-Àngel, R. Orús, and R. Zandbergen (2011), Comparative testing of four ionospheric models driven with GPS measurements, *Radio Sci.*, *46*, RS0D12, doi:10.1029/2010RS004584.

1. Introduction

[2] Many different models of the ionosphere have been developed over the last 50 years under the auspices of a wide range of national and international organizations; e.g., the International Telecommunications Union (ITU), the European Cooperation in Science and Technology (COST) program, and the International Union of Radio Science (URSI). These ionospheric models can be broadly classified into three main categories: (1) first principles models based on ionospheric physics and chemistry. They are generally referred to as "physical models"; (2) parametric models which simplify the physical models reducing the number of parameters; (3) empirical models based on observations.

[3] Physical models operate by solving a set of first principles continuity, energy, and momentum equations for the ionospheric plasma [*Schunk*, 1988; *Anderson*, 1993]. Two examples of such models are the Utah State University (USU) Time Dependent Ionospheric Model (TDIM) [*Schunk et al.*, 1986] and the University College London and Sheffield University Coupled Thermosphere-Ionosphere Model (CTIM) [*Fuller-Rowell et al.*, 1987; *Quegan et al.*, 1982]. Unfortunately, physical models require extensive computer resources to provide affordable run times. It should also be noted that physical models (especially ones that are not coupled to neutral atmosphere models) often require inputs derived from empirical models such as the Horizonal Wind Model (HWM) [e.g., *Hedin et al.*, 1996; *Drob et al.*, 2008].

[4] Parametric models simplify the physical models by parameterising them in terms of solar-terrestrial indices and geographical locations. They aim to give a realistic representation of the ionosphere's spatial and temporal structure using a limited number of numerical coefficients. Two examples of parametric models are the Fully Analytical Ionospheric Model (FAIM) [*Anderson et al.*, 1989] and the Parameterised Ionospheric Model (PIM) [*Daniell et al.*, 1993a, 1993b].

[5] Empirical models extract, in general, information on statistical systematic ionospheric variations from past data

[1]VEGA Space GmbH, Navigation Support Office, European Space Operations Centre, European Space Agency, Darmstadt, Germany.
[2]Centre for RF Propagation and Atmospheric Research, QinetiQ Ltd., Malvern, UK.
[3]Institute for Communication and Navigation, German Aerospace Centre, Neustrelitz, Germany.
[4]Research Group of Astronomy and Geomatics, Technical University of Catalonia, Barcelona, Spain.
[5]VITROCISET, Wave Interaction and Propagation Section, European Space Technology Centre, European Space Agency, Noordwijk, Netherlands.
[6]Navigation Support Office, European Space Operations Centre, European Space Agency, Darmstadt, Germany.

0048-6604/11/2010RS004584

records. They are often formulated in terms of monthly median parameters; hence they can describe long time average conditions of the ionosphere. This category of models includes the Bent Model [*Bent et al.*, 1972] and the International Reference Ionosphere (IRI) [*Bilitza*, 2001].

1.1. Assimilative Models

[6] In the last 15 years, there has been a rapid growth in the development and use of ionospheric "weather" models and other imaging techniques. There exists a wide range of very different approaches, but they can all be generally described as assimilative, since they aim to combine a background model with ionospheric measurements. Background models of assimilative models may range from physical models, through empirical models (e.g., IRI), to the use of closed form orthonormal functions. Assimilation techniques used include Kalman filtering, 3-D variational techniques and Tikhonov Regularisation. An excellent recent review of assimilation models can be found in the work of *Bust and Mitchell* [2008].

1.2. Paper Overview

[7] The results in this paper derive from a study initiated by the European Space Agency (ESA)/European Space Operations Centre (ESOC) in Darmstadt, Germany. Part of that study was to undertake comparative testing of four assimilative ionospheric models. The models were all provided with identical input data sets (consisting of ground and space based GPS measurements) and then tested against an independent truth data set considered as truth. The truth data included GPS dual frequency data, dual frequency altimeter data, ionosonde data and Langmuir probe data; however, in this paper we will focus on the results using GPS truth data.

[8] The rest of the paper is structured as follows: Section 2 describes some of the ionospheric modeling efforts undertaken at ESOC in order to set the current study in context. Brief descriptions of the four models under test are also provided. Section 3 provides a description of the input and truth data sets. Section 4 presents the results from the testing which are discussed in section 5. Conclusions are summarized in section 6.

2. Modeling Overview

2.1. Ionosphere Modeling at ESOC

[9] Since 1998, ESOC has been active as one of the four International GNSS Service (IGS) [*Beutler et al.*, 1999] Ionosphere Associate Analysis Centres (IAACs). The other IAACs are the Centre for Orbit Determination in Europe (CODE) at the University of Berne, Switzerland; the Jet Propulsion Laboratory (JPL) in the USA; and the Technical University of Catalonia (UPC) in Barcelona, Spain. Each IAAC independently computes rapid and final total electron content (TEC) maps which are then combined into a final IGS product. The TEC maps are global in extent and provided with a 2 h time resolution.

[10] ESOC maintains an interest in ionospheric modeling to support navigation applications (both terrestrial and spacecraft tracking) and other ESA missions that may require ionospheric corrections (e.g., the Soil Moisture and Ocean Salinity (SMOS) mission). It is anticipated that a number of enhancements will be required by ESOC (and other users) in future. These include: (1) the establishment of an effective ionospheric TEC prediction tool, (2) the availability of higher cadence TEC maps, (3) the ability to routinely incorporate observation data from new GNSS systems (such as Galileo) and from space based GNSS receivers, (4) the establishment of 3-D electron density reconstructions, and (5) the establishment of solar flare and traveling ionospheric disturbances (TIDs) monitoring techniques.

2.2. Models Under Comparison

[11] Four different ionospheric models that have been developed by members of the study team have been compared. These models are briefly described in the following sections, highlighting their key features and providing the relevant references. Moreover, two additional models have been included in the testing to provide a reference performance level. These are NeQuick and the IGS combined TEC product. Brief descriptions of these models are therefore also provided.

2.2.1. Electron Density Assimilative Model

[12] The Electron Density Assimilative Model (EDAM) has been developed by QinetiQ (UK) [*Angling and Khattatov*, 2006; *Angling and Cannon*, 2004] to assimilate measurements into a background ionospheric model. This background model is provided by IRI2007 [*Bilitza and Reinisch*, 2008] and the majority of the input data are total electron content (TEC) measurements derived from International GNSS Service (IGS) stations. Since the used IRI version does not include a plasmasphere, a simple exponential electron density profile, matched to the IRI scale height at 2000 km, is used above this height. The assimilation is based on a weighted, damped least mean squares estimation. This is a form of minimum variance optimal estimation (also referred to as Best Linear Unbiased Estimation (BLUE)) that provides an expression for an updated estimation of the state (known as the analysis) that is dependent upon an initial estimate of the state (the background model), and the differences between the background model and the observations [*Menke*, 1989; *Twomey*, 1977].

[13] Using the background model, electron densities are established on a 3-D grid of voxels in a magnetic coordinate system that remains fixed in space with respect to the Sun. Observed slant TEC measurements are simply expressed as sum of the electron densities of all voxels crossed by the slant range path of measurement. The relationship between the updated model (the analysis) and the background model is established by the difference between the observation vector and the observation operator which links the geometry of observations to the background model. Before being applied to the background model state, this difference is scaled with a weight matrix, which is composed of the error covariance matrices of the background model and the observables. For more details and algorithms about EDAM, see *Angling and Khattatov* [2006] and *Angling and Cannon* [2004].

[14] An assimilation time step of 15 min is used, and the electron density differences between the voxels of the analysis and the background are propagated from one time step to the next by assuming persistence combined with an exponential decay (damping). The time constant for this decay is set to 4 h.

[15] In addition to ground based slant TEC measurements, EDAM can assimilate a variety of other types of data: space

based TEC derived from GNSS data (both in a radio occultation geometry and using navigation antennas); space based TEC derived from dual frequency altimeters; virtual height profiles from ionosondes [*Angling et al.*, 2010]; and electron density data from in situ sensors. EDAM has been designed to provide products to a wide range of users; one example is the provision of high frequency (HF) propagation predictions [*Angling et al.*, 2009].

2.2.2. Ionosphere Monitoring Facility, Version 2

[16] The Ionosphere Monitoring Facility (IONMON, v2) is currently under development at ESA/ESOC and uses an analytic function approach to describe ionospheric structures by means of vertical profile functions combined with horizontal surface functions [*Feltens*, 2007]. The mathematical models include, among others, different types of profile functions; empirical models for height-dependent scale heights; and a TEC integrator. TEC data derived from dual-frequency GNSS data can be processed in combination with observed electron density profiles. Currently these are derived from radio occultation measurements; however, the inclusion of other sources such as ionosondes, is in principle possible.

[17] The intention of the analytical function approach was to be able to include some very simple physical features into the model and, in this way, allow for some physical interpretation of its output. This concept follows the techniques described by *Ching and Chiu* [1973] and *Chiu* [1975] where the vertical structure of the ionosphere is described as a sum of Chapman profiles, one for each layer E, F_1, F_2. Each profile function has its key parameters, such as maximum electron density and height of maximum electron density. These key parameters are, in turn, expressed by global surface functions, whose coefficients are then estimated. In this way it is possible to describe the ionosphere in three dimensions. From their nature, analytical function approaches are not as flexible as voxel approaches; i.e., their temporal and spatial resolution is limited. On the other hand, they do provide analytical expressions for the electron density at any point in space and consequently avoid any problems associated with voxel interpolation.

[18] IONMON v2 offers a selection of several types of profile functions. These include the Chapman profile and variants of it; for instance a series expansion of the Chapman profile whose coefficients can be fitted to observed electron density profiles. Currently the IONMON v2 has no background model of electron density but relies solely on the availability of observation data. In sparsely covered regions IONMON v2 thus displays poor performance. Concepts and algorithms to introduce a background model, combined with an assimilation of observation data, into the IONMON are under development.

2.2.3. Tomographic Ionosphere Model

[19] The development of the tomography approach used in the Tomographic Ionosphere model (TOMION) was started at UPC in the second half of the 1990s [*Hernández-Pajares et al.*, 1997, 1999; *Juan et al.*, 1997]. At that time, the main focus was to assess the feasibility of computing better TEC maps with a coarse tomography algorithm. TOMION has since been developed to provide several versions which are able to process ground based GNSS ionospheric data, GNSS LEO radio occultation data [*Hernández-Pajares et al.*, 1998, 2000a], GNSS geodetic data [*Hernández-Pajares et al.*, 2000b], and ionosonde data [*García-Fernández et al.*, 2003]. In real-time processing it is also possible to provide corrections for precise user positioning (Wide Area Real-Time Kinematic (WARTK)) [see *Hernández-Pajares et al.*, 2002, 2010]. Since 1998, TOMION has been used in the UPC Ionospheric Analysis Centre for the IGS [*Hernández-Pajares et al.*, 2009].

[20] The version of TOMION used in this study (v1.5) generates Global Ionospheric Maps (GIMs) of vertical TEC (vTEC) and includes an interpolation module using Kriging technique [*Orús et al.*, 2005]. The ionosphere is represented by two or more layers of voxels. In each voxel the electron density is assumed to be constant. No background model is used. The assimilation of data proceeds in three steps: (1) an initial fit is made to the ground based TEC data with a quite coarse resolution (4° latitude × 6° longitude voxel size) in which a first TEC model, together with the satellite and receiver differential code biases (DCBs), is estimated; (2) data gaps are filled using a modified Kriging interpolation technique to generate GIMs, assuming a certain stationary dependence of vTEC residual errors in terms of the distance, to compute every set of weights in the interpolation process, especially important in ocean and southern hemisphere regions with sparse ground based GPS data available. For Kriging interpolation, the residuals between observed vTEC (slant TEC of the first fit and mapped to the vertical) and modeled vTEC (from the model of the first fit) are computed. Then by Kriging interpolation over these residuals, an accurate high resolution TEC map can be created. The interpolation weights are computed assuming a certain vTEC error decorrelation function on the distance, adjusted from previous runs. The procedure is described in more detail in section 5. In the second run the resolution can be reduced to 2°.5 latitude × 5° longitude and 15 min time intervals; and (3) an enhanced Abel Transform retrieval is used to produce high accuracy and high resolution electron density fields in the vicinity of radio occultation measurements, by taking the previous vTEC as a proxy of the horizontal gradients in the occultation region. Presently new optimized versions of TOMION, for real-time and predicted VTEC maps, are continuously running in the context of IGS real-time and ionospheric working groups, respectively.

2.2.4. Neustrelitz TEC Models

[21] GNSS based TEC monitoring has been carried out at the German Aerospace Centre (DLR, Neustrelitz, Germany) on a routine basis since 1995. TEC maps have been produced over Europe with a temporal resolution of 10 min [*Jakowski*, 1996] using input data provided mainly by the European IGS network. The resulting database of TEC maps covers more than a full solar cycle.

[22] Underpinning the DLR real time TEC maps is a family of empirical TEC models (Neustrelitz TEC Models, NTCM) that have been developed for the European (-EU) [e.g., *Jakowski et al.*, 1998] and both polar areas (-NP and –SP). Recently a global TEC model has also been established [*Jakowski et al.*, 2011]; however, in this study only TEC maps covering the European area have been used. The regional European vTEC is described by the NTCM with a polynomial of 60 linear terms [*Jakowski*, 1996] representing the diurnal and semidiurnal variation, the annual and semiannual variation, the dependence on the latitude and the solar zenith angle, and the dependence on the solar activity. Some of these polynomial terms reflect ionospheric/thermospheric

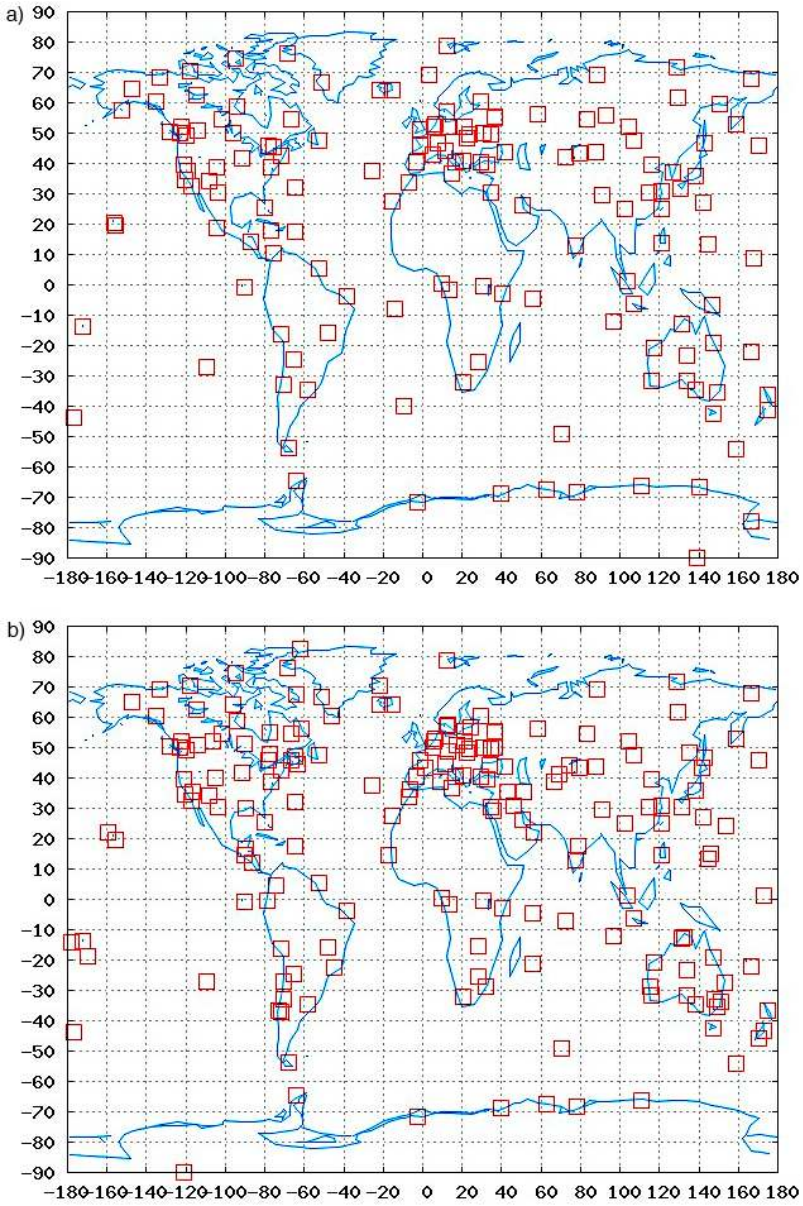

Figure 1. (a) Input GPS stations for May 2002. (b) Input GPS stations for December 2006.

relationships. The solar activity level dependence is controlled by the solar radio flux index F10.7. The model coefficients are deduced from calibrated GPS TEC measurements by a least square fitting procedure.

[23] The TEC data used in this study were obtained after assimilating the measured GPS TEC into the NTCM-EU background TEC model as described by *Jakowski* [1996, 1998]. Each grid point in the TEC maps is formed from a weighted mean of the differences between the nearest measured and modeled vTEC values [*Jakowski*, 1998]. For each measurement point Gauss functions are used to compute a weight decaying exponentially with increasing distance from that measurement point. Grid spacing for the European area is 2.5° latitude × 5° longitude. A single layer mapping function is used to convert the measured slant TEC to vertical. The ionospheric height is fixed at 400 km.

2.2.5. Nequick

[24] NeQuick [*Radicella*, 2009; *Hochegger et al.*, 2000; *Radicella and Leitinger*, 2001; *Nava et al.*, 2008] is a monthly median 3-D ionospheric model that uses a sum of Epstein layers to produce an analytic function describing the ionospheric electron density distribution. The construction of the electron density profile is based on anchor points related to standard ionospheric characteristics (i.e., $foF2$, $M(3000)F2$, $foF1$, foE). It has been designed so that the electron density profile and its first derivative are always continuous.

[25] NeQuick is the official ionosphere correction model incorporated in Galileo receivers [*Galileo Information Center*, 2006] and the model coefficients are broadcast as part of the Galileo navigation message. The model has also been adopted as an ITU standard [*ITU-R*, 2007].

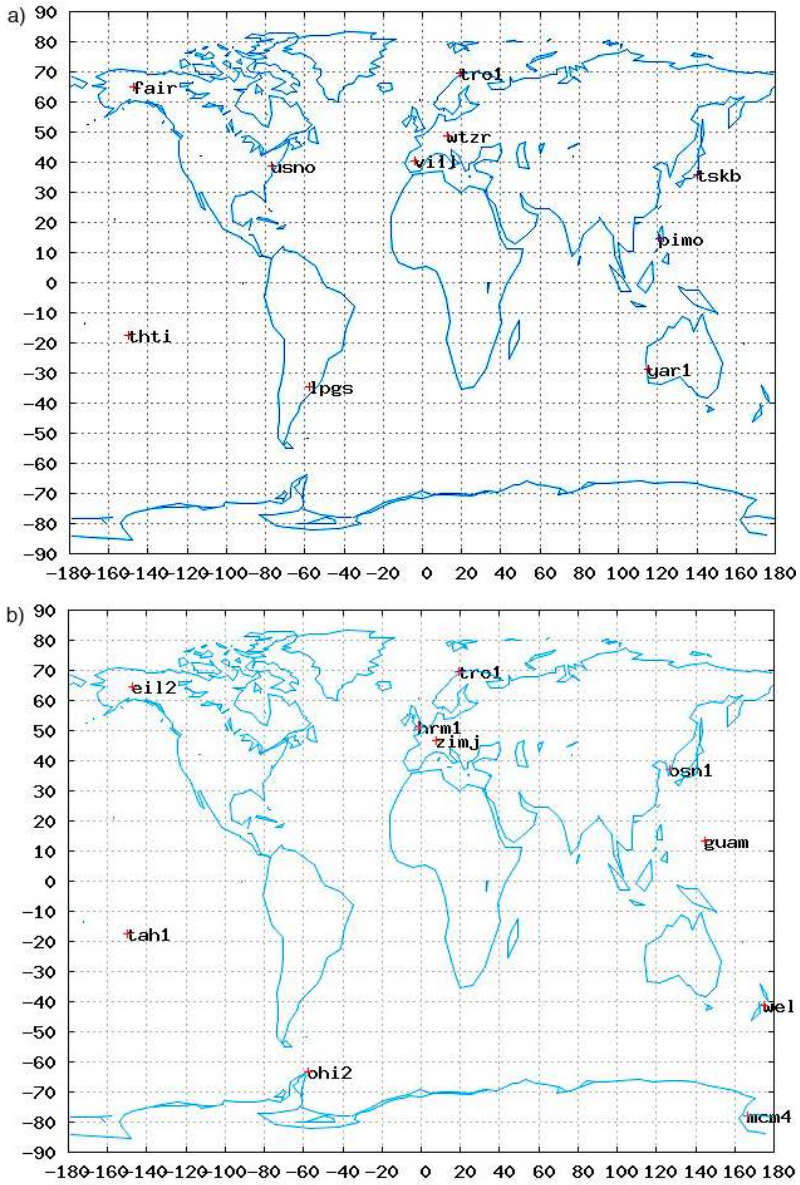

Figure 2. (a) Test GPS stations for May 2002. (b) Test GPS stations for December 2006.

2.2.6. IGS Combined TEC Product

[26] The IGS TEC maps [*Hernández-Pajares et al.*, 2009; *Krankowski et al.*, 2010] are produced routinely by the IGS with 11 days latency in final mode and with 1 day latency in rapid mode. Daily predicted IGS TEC maps are currently produced in an experimental mode. Four analysis centers, the so-called IAACs (CODE, ESOC, JPL, UPC, see section 2.1), produce with their individual modeling techniques global TEC maps on a 2.5° latitude × 5° longitude grid with a 2 h time resolution. These are delivered to the IGS using IONEX format [*Schaer et al.*, 1998]. The IGS combined TEC maps are then established as weighted means of the individual TEC maps delivered by the four centers. For the computation of the weights, the individual IAAC TEC maps are validated against observed slant TEC data recorded at selected GPS stations. Thus the IGS TEC maps should not be understood as a conventional "ionosphere model" but as resulting from weighted mean computations of TEC maps produced by different analysis centers with their individual modeling techniques. The TEC accuracy is considered to be in the order of a few TECu (1 TECu = 1×10^{16} electrons/m^2) in regions well covered with GNSS receivers (see Figure 10 of *Hernández-Pajares* [2004]).

3. Data Sets

3.1. Test Periods

[27] Two test periods were chosen for the study. Each was one month long and they were selected in order to sample both solar maximum and solar minimum conditions. The first period comprised May 2002, when the 12 month running sunspot number (SSN) was 108.8. The second period was December 2006, when the SSN was 12.1. Both test periods

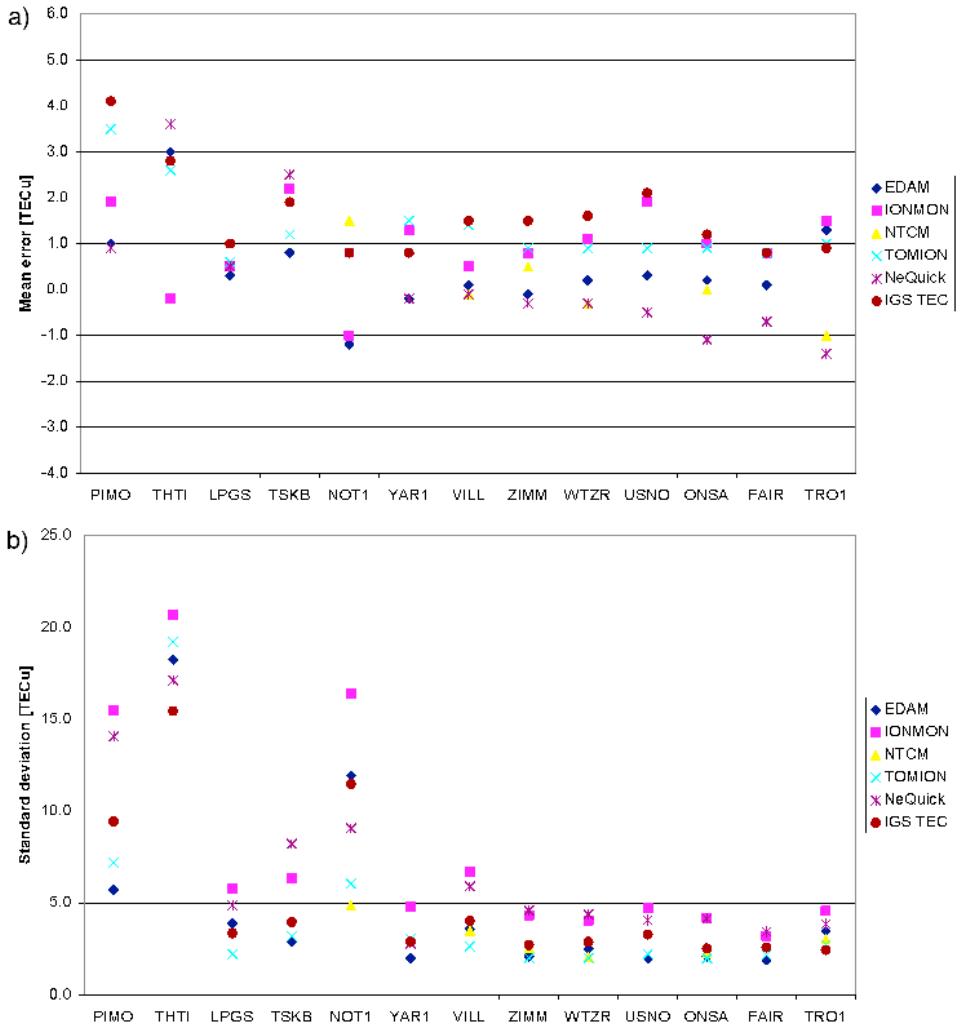

Figure 3. May 2002 nighttime results. (a) Mean errors and (b) the standard deviation of the TECu error. N.B. stations are ordered by geomagnetic latitude.

display widely varying geomagnetic activity levels with *Kp* index values ranging from 0 to 9.

3.2. Input Data

[28] A unified set of input data was provided to each of the four models under test. The data consisted of:

[29] 1. Daily RINEX data files containing data from ground based GPS receivers with a 30 s measurement sampling rate. Due to changes in the availability of data, 151 IGS ground sites were used for the May 2002 test (Figure 1a) and 190 IGS sites were used for the December 2006 test (Figure 1b). The station locations were chosen to provide a worldwide distribution of data with a reasonable level of homogeneity.

[30] 2. Space based GPS data were also provided. For the May 2002 test, CHAMP and SAC-C data were used, while for the December 2006 data from the FORMOSAT-3/COSMIC satellite constellation were used.

3.3. Test Data

[31] In all, four types of test data were used: differential slant TEC, absolute vertical TEC, foF2/hmF2 from ionosondes, and in situ electron density measurements from CHAMP. This paper is restricted to the presentation of the results from the differential slant TEC data.

[32] Due to differential code biases (DCBs) in the GPS transmitters and receivers it is not possible to derive truly absolute TEC values from GPS measurements. However, over a phase continuous measurement arc, GPS can measure differential TEC to an accuracy of less than 0.1 TECu. Therefore, differential slant GPS TEC (dSTEC) has been used for the model validations. The dSTEC was defined as the difference between slant TEC measured at any point along a continuous-phase arc and the slant TEC measured when the GPS satellite is at its highest elevation (i.e., close enough to be a vertical TEC estimate) seen from a given receiver. Since the whole measurement does not occur instantaneously, the dSTEC incorporates contributions from both spatial and temporal variations within the ionosphere. As such it provides a good test of an ionospheric model including mapping function assessment. The test data was limited to a 15° elevation cutoff and provided at 5 min intervals. The results have been split between 06:00–17:59 LT (i.e., local day) and 18:00–05:59 LT (i.e., local night) with respect to the high elevation

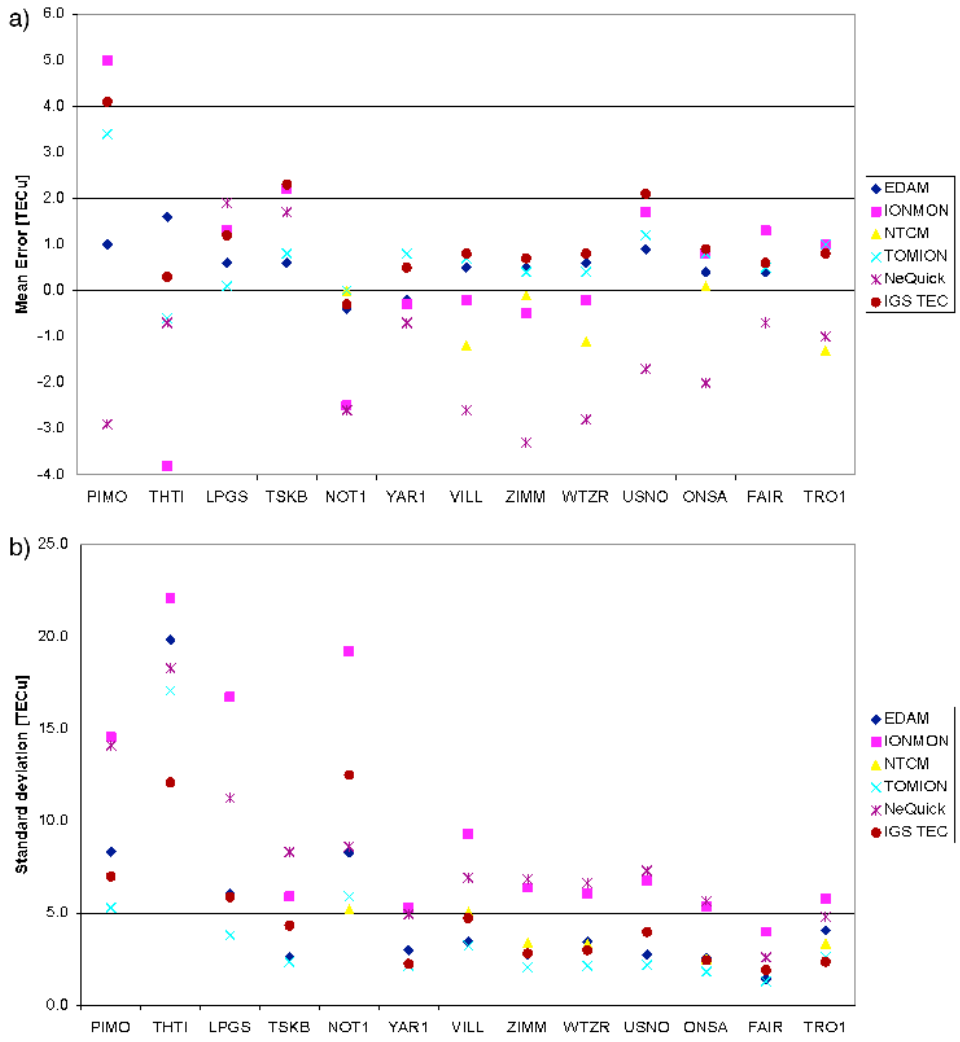

Figure 4. May 2002 daytime results. (a) Mean errors and (b) the standard deviation of the TECu error. N.B. stations are ordered by geomagnetic latitude.

reference. The independent test stations that have been used are shown in Figures 2a and 2b.

4. Intercomparison Results

[33] The mean dSTEC error and the standard deviations of the dSTEC are shown in Figures 3–6. The results are divided into local day and local night and are presented for May 2002 and December 2006. Each vertical column of the plots shows the results from the six models under test for a particular GPS station that is indicated by its four character identifier. In each plot the stations are ordered by geomagnetic latitude that increases from left to right.

[34] For all the models, except the IGS combined product (IGS-TEC), the test stations have not been included in the assimilation (i.e., they form an independent test set). In order to assess possible effects of analyzing postfit residuals, the above described dSTEC validations were also repeated for all models with three IGS sites whose GPS data entered into the model fits (May 2002: NOT1, ZIMM, ONSA; December 2006: NOT1, TLSE, ONSA). Figures 3–6 show that there is not a distinct difference between the models' results from the two classes of midlatitude test receiver, apart from NOT1 (Noto at Sicily/Italy) which displays very large standard deviations of up to 20 TECU for the May 2002 solar maximum test period (Figures 3 and 4).

[35] The overall trends within the results are generally as expected: (1) The daytime absolute errors tend to be larger than the nighttime errors. (2) The errors for the high sunspot period (May 2002) are larger than for the low sunspot period (December 2006). Note the change in scales between the two periods in the corresponding figures. (3) Errors from midlatitude stations are generally lower than those from low and high latitudes. (4) The greatest errors occur at stations that are both low latitude and isolated from the input test data (i.e., THTI and TAH1).

[36] The results for NOT1 (Noto at Sicily/Italy) during the high sunspot number period (May 2002) display standard deviations comparable to those of THTI and TAHI. A closer analysis of the NOT1 dSTEC data revealed the existence of large dSTEC values for low elevation southerly measurements; below 30° dSTEC values up to 100 TECu are observed, while below 10° values up to 250 TECu are observed. These large dSTEC values may indicate the existence of large gradients in the equatorial ionosphere which were not properly

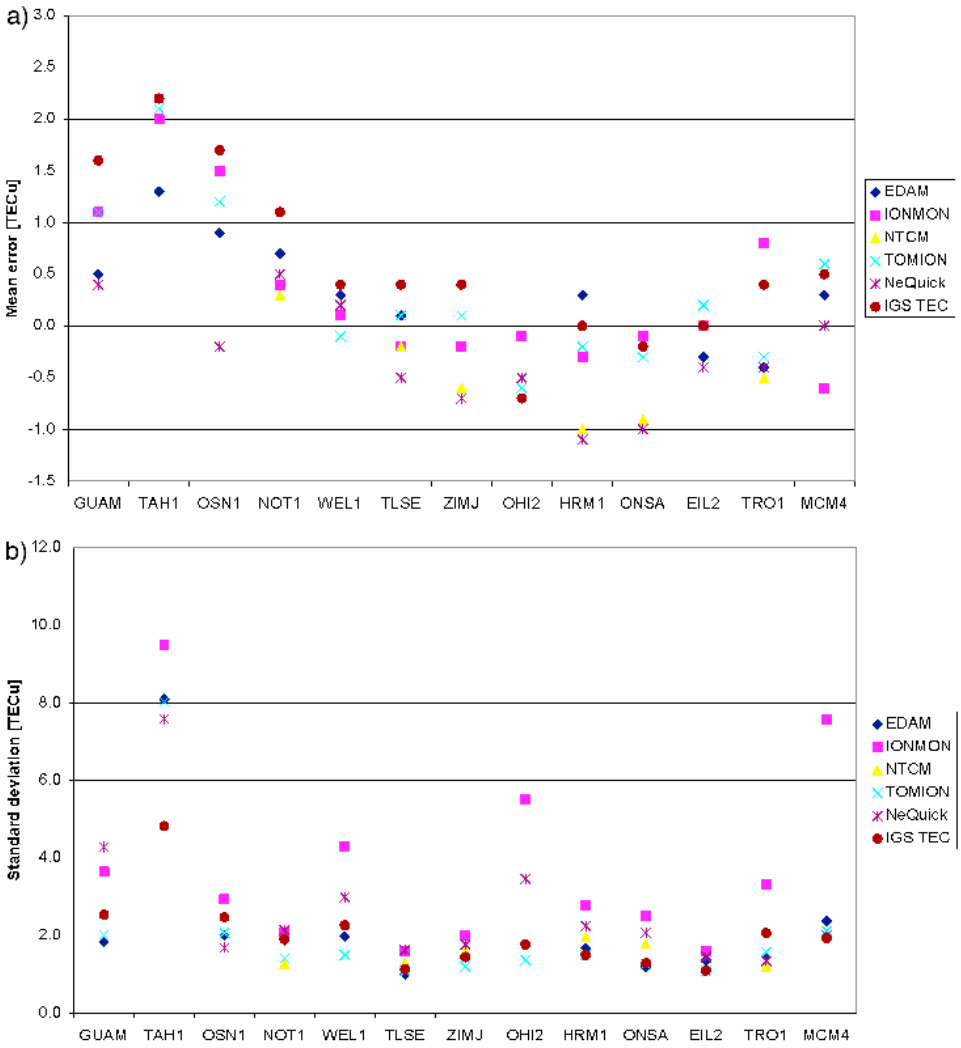

Figure 5. December 2006 nighttime results. (a) Mean errors and (b) the standard deviation of the TECu error. N.B. stations are ordered by geomagnetic latitude.

represented by any of the tested models, probably due to the poor data coverage over the African region.

[37] For midlatitude stations, the dSTEC standard deviations are generally around 1.5 TECu for EDAM, NTCM, TOMION and IGS-TEC for the high sunspot period (May 2002) and within 1 TECu for the low sunspot number period (December 2006). The lowest reported standard deviation across all models and all stations is 0.99 TECu (EDAM, TLSE station for December 2006 night). Overall however, the best performing model is TOMION which provides the lowest standard deviation for 6 out of 13 stations for May 2002 (night), 10 out of 13 stations for May 2002 (day), 5 out of 13 stations for December 2006 (night) and 7 out of 13 stations for December 2006 (day).

[38] IONMON consistently displays the worst standard deviations of the assimilative models. The reasons for this will be discussed in the following section.

5. Discussion

[39] The way the dSTEC tests were formulated provides a stringent test of a model's ability to capture both spatial and temporal gradients in the ionosphere. Of the models reported here only TOMION has a technique to take into account the empirical vTEC error decorrelation, as a certain function of the distance (for instance including the exponential), in order to consistently compute the optimal weights for each interpolation point, based on the distribution of the data set (for details, see *Orús et al.* [2005], in particular variogram definition and use on pages 2 and 3). It is probably this approach in which TOMION takes into account the error decorrelation, assuming its dependence mainly in terms of the distance, which is the main modeling difference that results in TOMION having the best overall performance. This point is consistent with similar results obtained in the overall study; TOMION provides excellent results when compared with vTEC data independently derived from dual-frequency altimeter data. This data is only available over the oceans where the interpolation/extrapolation techniques used in the modeling play a central role.

[40] The sensitivity of the testing to model gradients can also be evidenced in results from EDAM. The results presented in Figures 3–6 have been derived by taking the EDAM

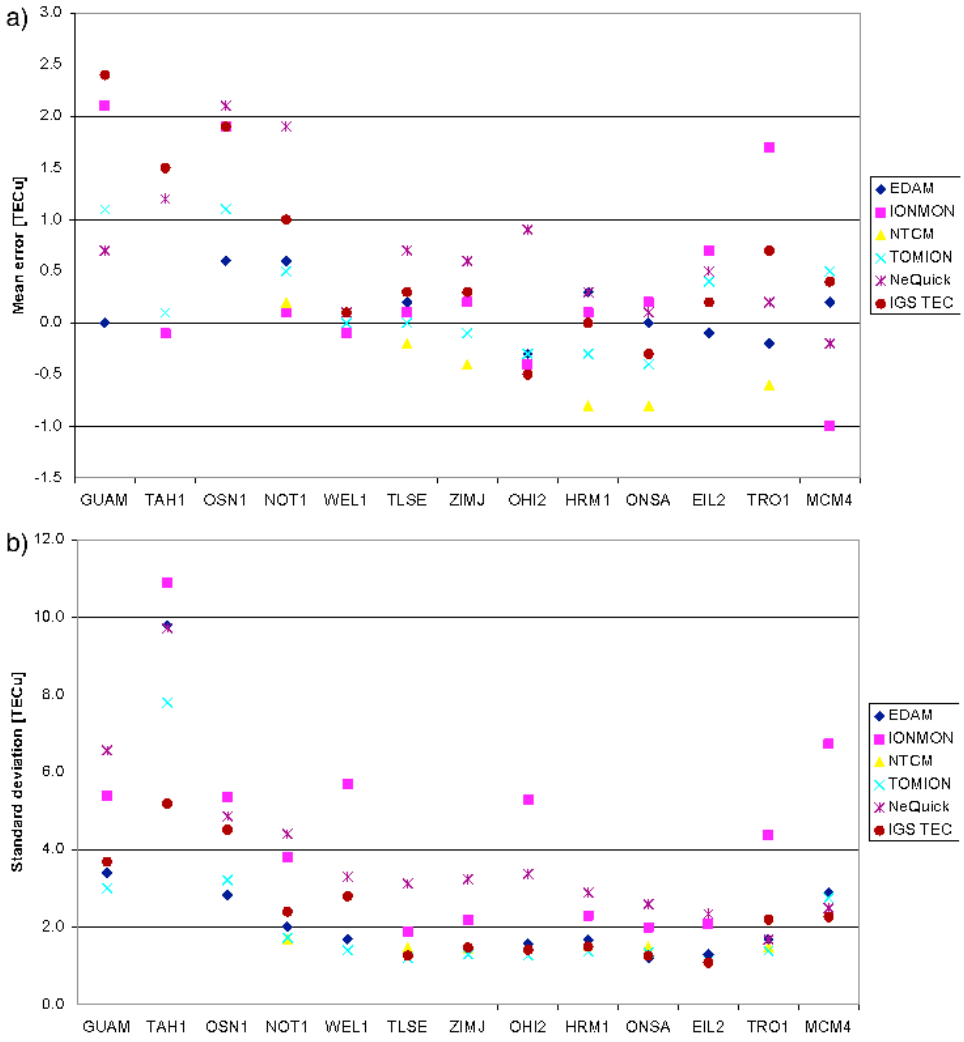

Figure 6. December 2006 daytime results. (a) Mean errors and (b) the standard deviation of the TECu error. N.B. stations are ordered by geomagnetic latitude.

electron density grid, which is natively in geomagnetic coordinates, and interpolated onto a geographic grid before the differential slant TECs are estimated. An alternative approach is to convert the end points of the dSTEC truth data to geomagnetic coordinates and then extract the dSTECs directly from the geomagnetic EDAM grid. The first approach naturally applies some smoothing to the electron density grid as part of the interpolation process, while the second approach does not. For the low sunspot period (December 2006) the second approach significantly reduces the dSTEC errors; for example the dSTEC standard deviation for the HRM1 station at night reduces from 1.7 TECu to 1.3 TECu. This indicates that, for this period, ionospheric gradients are being well modeled and the dSTEC results are being degraded by the additional smoothing. Conversely, in the high sunspot period (May 2002) results are worse when the smoothing is not applied (e.g., changing from 3.5 TECu to 4.2 TECu for TRO1 at night), indicating that the model may have over estimated the ionospheric gradients. It should be noted that the same model of distance dependencies has been used by the EDAM assimilation algorithm for both periods; it seems clear that considering the vTEC error decorrelation dependence in terms of the distance, as displayed in TOMION, would be beneficial.

[41] Since the NTCM based TEC map reconstruction uses a single layer approach for the mapping function, the accuracy of transforming vertical to slant TEC measurements (dSTEC) and vice versa is in principle restricted. This limitation is acceptable given the requirement to produce robust and reliable TEC maps in near real time (see http://swaciweb.dlr.de). The NTCM maps display errors that are consistent with EDAM and TOMION. The good performance is not surprising given that long-term testing has demonstrated that RMS deviations of the NTCM-EU background model for vertical TEC from corresponding monthly medians are less than 1 TECU under low solar activity conditions and less than 3 TECU under high solar activity conditions.

[42] IONMON v2, in its current setup, has no background model and relies solely on observational data to constrain the model parameters. Such an approach leaves the model vulnerable to degradation when insufficient data is available. In particular, the lack of vertical profile information from radio

occultation or ionosondes is detrimental to its performance. The effect of the sparseness of the input data is most apparent in the May 2002 results, where the IONMON v2 results are considerably worse than the other assimilative models. Furthermore, due to limitations in the current implementation, the IONMON v2 3-D grid is collapsed into a 2-D TEC map for testing against the truth data. To assess the effect that this approach may have, a small number of comparisons have been made with IONMON version 1 (v1). IONMON v1 is a well developed single layer model used operationally for ESOC's contributions to the International GNSS Service (IGS) Ionosphere Working Group and to support in-house missions. It is a single layer (i.e., thin shell) model of the ionosphere and represents the global TEC using spherical harmonics. It was found that, in general, the dSTEC mean errors of IONMON v2 were about twice as large as those of v1, and the dSTEC standard deviations of v2 were around factor 1.3 larger than those of v1. Since the v2 model should in principle be able to perform at least as well as the v1 model, further investigations are ongoing. Steps are currently being undertaken to include a background model combined with an assimilation technique in order to stabilize the fits.

6. Conclusions

[43] Four ionospheric models (the Electron Density Assimilative Model, EDAM; the Ionosphere Monitoring Facility, IONMON v2; the Tomographic Ionosphere model, TOMION; and the Neustrelitz TEC Models, NTCM) have been run using a controlled set of input data. Each model output has been tested against differential slant TEC (dSTEC) truth data for a high (May 2002) and low (December 2006) sunspot period.

[44] Three of the models (EDAM, TOMION and NTCM) produce dSTEC standard deviation results that are broadly consistent with each other. Note that the dSTEC standard deviation provides a measure of how well a model can track changes in the truth dSTEC while neglecting biases. The dSTEC standard deviations for these three models agree with respect to each other to ~1 TECu for December 2006 and to ~1.5 TECu for May 2002, apart from a few exceptions, e.g., NOT1. The model with the best overall dSTEC performance is TOMION which has the lowest standard deviation in 28 out of 52 test cases (13 stations, two test periods, day and night). This is probably due to the adapted Kriging technique used in TOMION. The lowest reported standard deviation across all models and all stations was 0.99 TECu (EDAM, TLSE station for December 2006 night).

[45] The reviewed models involve different types of data driven reconstructions of TEC with different priority goals. Similar accuracy results indicate clearly the level of accuracy that can be reached nowadays in TEC reconstructions by utilizing commonly available data sources. To make essential progress in improving the accuracy and temporal/spatial resolution of TEC reconstructions the authors see two main directions for further developments: (1) In the medium term, empirical modeling: reconstructions of the 3-D electron density distribution by sophisticated tomographic methods and assimilation of observation data into well qualified empirical 3-D models. (2) In the long-term, physics based modeling: data driven physics based numerical models having the capability to forecast the ionospheric behavior and to fill remaining data gaps.

[46] In both cases the reconstructions require comprehensive data sets. This is a condition that permanently improves, e.g., by rapidly growing ground based GNSS networks, a growing number of space based GNSS measurements on LEO satellites such as COSMIC, and the availability of several GNSS such as GPS, GLONASS, Galileo and others that are currently established.

[47] **Acknowledgments.** The results in this paper were derived from the Study "GNSS Contribution to Next Generation Global Ionospheric Monitoring" initiated by the European Space Agency (ESA)/European Space Operations Centre (ESOC), Darmstadt, Germany. The study was funded by ESA's Technical Research Programme (TRP). The authors thank IGS for making available high-quality GPS observation data and Matthias Foerster for providing electron density data from CHAMP. EDAM has been developed under funding from the UK Ministry of Defense Science and Technology program. Recent UPC updates of TOMION have been partially supported by the Spanish Ministry of Science and Innovation, under the ESP2007–62676 and CTM2010-21312-C03-02 projects.

References

Anderson, D. N. (1993), Global ionospheric modelling, in *Modern Radio Science*, edited by H. Matsumoto, Oxford Univ. Press, New York.

Anderson, D. N., J. M. Forbes, and M. Codrescu (1989), A fully analytical, low- and middle-latitude ionospheric model, *J. Geophys. Res.*, *94*, 1520.

Angling, M. J., and P. S. Cannon (2004), Assimilation of radio occultation measurements into background ionospheric models, *Radio Sci.*, *39*, RS1S08, doi:10.1029/2002RS002819.

Angling, M. J., and B. Khattatov (2006), Comparative study of two assimilative models of the ionosphere, *Radio Sci.*, *41*, RS5S20, doi:10.1029/2005RS003372.

Angling, M. J., J. Shaw, A. K. Shukla, and P. S. Cannon (2009), Development of an HF selection tool based on the Electron Density Assimilative Model near-real-time ionosphere, *Radio Sci.*, *44*, RS0A13, doi:10.1029/2008RS004022 [printed *45*(1), 2010].

Angling, M. J., P. S. Cannon, and N. K. Jackson-Booth (2010), On the assimilation of collocated and concurrent data from ionosondes and GPS receivers, paper presented at Beacon Satellite Symposium, Int. Union of Radio Sci., Barcelona, Spain.

Bent, R. B., S. K. Llewllyn, and P. E. Schmid (1972), Ionospheric refraction corrections in satellite tracking, *Space Res.*, *12*, 1186–1194.

Beutler, G., M. Rothacher, S. Schaer, T. A. Springer, J. Kouba, and R. E. Neilan (1999), The International GPS Service (IGS): An interdisciplinary service in support of Earth sciences, *Adv. Space Res.*, *23*(4), 631–635.

Bilitza, D. (2001), International Reference Ionosphere 2000, *Radio Sci.*, *36*, 261–275.

Bilitza, D., and B. W. Reinisch (2008), International Reference Ionosphere 2007: Improvements and new parameters, *J. Adv. Space Res.*, *42*(4), 599–609.

Bust, G. S., and C. N. Mitchell (2008), History, current state, and future directions of ionospheric imaging, *Rev. Geophys.*, *46*, RG1003, doi:10.1029/2006RG000212.

Ching, B. K., and Y. T. Chiu (1973), A phenomenological model of global ionospheric electron density in the E-, F1-, and F2-regions, *J. Atmos. Terr. Phys.*, *35*, 1615.

Chiu, Y. T. (1975), An improved phenomenological model of ionospheric density, *J. Atmos. Terr. Phys.*, *37*, 1563–1570.

Daniell, R. E., W. G. Whartenby, and L. D. Brown (1993a), Parameterised Real-time Ionospheric Specification Model, PRISM version 1.2, Algorithm description, Comput. Phys., Inc., Newton, Mass.

Daniell, R. E., W. G. Whartenby, and L. D. Brown (1993b), Parameterised Real-time Ionospheric Specification Model, PRISM version 1.2, Validation report, Comput. Phys., Inc., Newton, Mass.

Drob, D. P., et al. (2008), An empirical model of the Earth's horizontal wind fields: HWM07, *J. Geophys. Res.*, *113*, A12304, doi:10.1029/2008JA013668.

Feltens, J. (2007), Development of a new three-dimensional mathematical ionosphere model at European Space Agency/European Space Operations Centre, *Space Weather*, *5*, S12002, doi:10.1029/2006SW000294.

Fuller-Rowell, T. J., D. Rees, S. Quegan, R. J. Moffett, and G. J. Bailey (1987), Interaction between neutral thermosphere composition and the

polar ionosphere using a coupled ionosphere-thermosphere model, *J. Geophys. Res.*, *92*, 7744.

Galileo Information Center (2006), Galileo open service signal in space interface control document, draft 0, *OS SIS ICD*, São José dos Campos, Brazil, 23 May.

García-Fernández, M., M. Hernández-Pajares, J. M. Juan, J. Sanz, R. Orús, P. Coisson, B. Nava, and S. M. Radicella (2003), Combining ionosonde with ground GPS data for electron density estimation, *J. Atmos. Sol. Terr. Phys.*, *65*, 683–691.

Hedin, A. E., et al. (1996), Empirical wind model for the upper, middle and lower atmosphere, *J. Atmos. Terr. Phys.*, *58*, 1421–1447.

Hernández-Pajares, M. (2004), IGS ionosphere WG status report: Performance of IGS ionosphere TEC maps, position paper presented at IGS Workshop, Int. GPS Serv., Bern.

Hernández-Pajares, M., J. M. Juan, and J. Sanz (1997), Neural network modeling of the ionospheric electron content at global scale using GPS data, *Radio Sci.*, *32*(3), 1081–1089, doi:10.1029/97RS00431.

Hernández-Pajares, M., J. M. Juan, J. Sanz, and J. G. Solé (1998), Global observation of the ionospheric electronic response to solar events using ground and LEO GPS data, *J. Geophys. Res.*, *103*(A9), 20,789–20,796.

Hernández-Pajares, M., J. M. Juan, and J. Sanz (1999), New approaches in global ionospheric determination using ground GPS data, *J. Atmos. Sol. Terr. Phys.*, *61*, 1237–1247.

Hernández-Pajares, M., J. M. Juan, and J. Sanz (2000a), Improving the Abel inversion by adding ground GPS data to LEO radio occultations in ionospheric sounding, *Geophys. Res. Lett.*, *27*(16), 2473–2476.

Hernández-Pajares, M., J. M. Juan, J. Sanz, and O. L. Colombo (2000b), Application of ionospheric tomography to real-time GPS carrier-phase ambiguities resolution at scales of 400–1000 km and with high geomagnetic activity, *Geophys. Res. Lett.*, *27*(13), 2009–2012.

Hernández-Pajares, M., J. M. Juan, J. Sanz, and O. L. Colombo (2002), Improving the real-time ionospheric determination from GPS sites at very long distances over the equator, *J. Geophys. Res.*, *107*(A10), 1296, doi:10.1029/2001JA009203.

Hernández-Pajares, M., J. M. Juan, J. Sanz, R. Orús, A. García-Rigo, J. Feltens, A. Komjathy, S. Schaer, and A. Krankowski (2009), The IGS VTEC maps: A reliable source of ionospheric information since 1998, *J. Geod.*, doi:10.1007/s00190-008-0266-1.

Hernández-Pajares, M., et al. (2010), Wide-area RTK: High precision positioning on a continental scale, *Inside GNSS*, March–April.

Hochegger, G., B. Nava, S. M. Radicella, and R. Leitinger (2000), A family of ionospheric models for different uses, *Phys. Chem. Earth Part C*, *25*(4), 307–310.

ITU-R (2007), Ionospheric propagation data and prediction methods required for the design of satellite services and systems, *ITU-R P 531–9*, Geneva, Switzerland.

Jakowski, N. (1996), *TEC Monitoring by Using Satellite Positioning Systems, Modern Ionospheric Science*, edited by H. Kohl, R. Rüster, and K. Schlegel, pp. 371–390, ProduServ GmbH, Berlin.

Jakowski, N. (1998), Generation of TEC maps over the COST area based on GPS measurements, paper presented at 2nd COST251 Workshop, Side, Turkey, 30–31 March.

Jakowski, N., E. Sardon, and S. Schlueter (1998), GPS-based TEC observations in comparison with IRI95 and the European TEC model NTCM2, *Adv. Space Res.*, *22*, 803–806.

Jakowski, N., M. M. Hoque, and C. Mayer (2011), A new global TEC model for estimating transionospheric radio wave propagation errors, *J. Geod.*, in press.

Juan, J. M., A. Rius, M. Hernández-Pajares, and J. Sanz (1997), A two-layer model of the ionosphere using Global Positioning System data, *Geophys. Res. Lett.*, *24*(4), 393–396.

Krankowski, A., M. Hernández-Pajares, J. Feltens, A. Komjathy, S. Schaer, A. García-Rigo, and P. Wielgosz (2010), Present and future IGS Ionospheric products, paper presented at IGS Workshop, Int. GPS Serv., Newcastle upon Tyne, U. K., 28 June to 2 July.

Menke, W. (1989), *Geophysical Data Analysis: Discrete Inverse Theory*, Academic, San Diego, Calif.

Nava, B., P. Coisson, and S. M. Radicella (2008), A new version of the NeQuick ionosphere electron density model, *J. Atmos. Sol. Terr. Phys.*, *70*, 1856–1862.

Orús, R., M. Hernández-Pajares, J. M. Juan, and J. Sanz (2005), Improvement of global ionospheric VTEC maps by using Kriging interpolation technique, *J. Atmos. Sol. Terr. Phys.*, *67*(16), 1598–1609.

Quegan, S., G. J. Bailey, R. J. Moffett, R. A. Heelis, T. J. Fuller-Rowell, D. Rees, and R. W. Spiro (1982), A theoretical study of the distribution of ionization in the high-latitude ionosphere and the plasmasphere: First results on the midlatitude trough and the light-ion trough, *J. Atmos. Terr. Phys.*, *44*, 619.

Radicella, S. M. (2009), The NeQuick model genesis, uses and evolution, *Ann. Geophys.*, *52*(3/4).

Radicella, S. M., and R. Leitinger (2001), The evolution of the DGR approach to model electron density profiles, *Adv. Space Res.*, *27*, 35–40.

Schaer, S., W. Gurtner, and J. Feltens (1998), IONEX: The Ionosphere Map Exchange Format Version 1, paper presented at the IGS Analysis Center Workshop, Int. GNSS Serv., Darmstadt, Germany, 9–11 Feb.

Schunk, R. W. (1988), A mathematical model of the middle and high latitude ionosphere, *Pure Appl. Geophys.*, *127*, 255.

Schunk, R. W., J. J. Sojka, and M. D. Bowline (1986), Theoretical study of the electron temperature in the high latitude ionosphere for solar maximum and winter conditions, *J. Geophys. Res.*, *91*, 12,041.

Twomey, S. (1977), *Introduction to the Mathematics of Inversion in Remote Sensing and Indirect Measurements*, Dover, New York.

M. Angling and N. Jackson-Booth, Centre for RF Propagation and Atmospheric Research, QinetiQ Ltd., Malvern WR14 3LG, UK. (mjangling@qinetiq.com)

A. Aragón-Àngel and M. Hernández-Pajares, Research Group of Astronomy and Geomatics, Technical University of Catalonia, C/Jordi Girona 1-3, Campus Nord, Edificio C3, Despacho 209, E-08034 Barcelona, Spain. (manuel@ma4.upc.edu)

J. Feltens, VEGA Space GmbH, Navigation Support Office, European Space Operations Centre, European Space Agency, Robert-Bosch-Strasse 5, D-64293 Darmstadt, Germany. (joachim.feltens@esa.int)

M. Hoque and N. Jakowski, Institute for Communication and Navigation, German Aerospace Centre, Kalkhorstweg 53, D-17235 Neustrelitz, Germany. (norbert.jakowski@dlr.de)

R. Orús, VITROCISET, Wave Interaction and Propagation Section, European Space Technology Centre, European Space Agency, Keplerlaan 1, NL-2201 AZ Noordwijk ZH, Netherlands. (raul.orus.perez@esa.int)

R. Zandbergen, Navigation Support Office, European Space Operations Centre, European Space Agency, Robert-Bosch-Strasse 5, D-64293 Darmstadt, Germany. (rene.zandbergen@esa.int)